Journal of Microscopy

*Journal of Microscopy, 2011*
*Received 15 February 2011; accepted 15 September 2011*

doi: 10.1111/j.1365-2818.2011.03565.x

# Asynchronous event-based high speed vision for microparticle tracking

Z. NI, C. PACORET, R. BENOSMAN, S. IENG, & S. RÉGNIER
*Institut des Systèmes Intelligents et de Robotique, UPMC, CNRS UMR-7222, 4 place Jussieu, CC 173, 75252 Paris cedex 05, France.*

**Key words.** Address-event representation (AER), Brownian motion, high speed vision, Hough transform, microrobotics, particle tracking.

## Summary

This paper presents a new high speed vision system using an asynchronous address-event representation camera. Within this framework, an asynchronous event-based real-time Hough circle transform is developed to track microspheres. The technology presented in this paper allows for a robust real-time event-based multiobject position detection at a frequency of several kHz with a low computational cost. Brownian motion is also detected within this context with both high speed and precision. The carried-out work is adapted to the automated or remote-operated microrobotic systems fulfilling their need of an extremely fast vision feedback. It is also a very promising solution to the micro physical phenomena analysis and particularly for the micro/nanoscale force measurement.

## Introduction

Control is a fundamental challenge at the microscopic scale. At this scale, the volumetric forces are indeed negligible compared to the surface forces and dynamic effects are dominant because of weak masses and inertia. Two important issues could be addressed: trajectory control of high speed autonomous microrobots in constrained environments (Ivan *et al.,* 2011) and force-feedback high-resolution telemanipulation (Pacoret *et al.,* 2009, 2010; Bolopion *et al.,* 2010). The use of smart materials such as piezoelectric actuators provides adequate accuracy but introduces very high dynamics that are not easily controlled. Robust and ultrafast tracking of microobjects in large workspaces is required in order to implement closed-loop control schemes. In this context, a sampling frequency of at least 1 kHz is required for the stability. Today, available sensors with desired specifications are either offline or of low resolution (reduced size of acquisition). Moreover, image processing techniques able to match this frequency are few and are not robust to the disturbances. The resulting lack of robust control schemes confine microsystems to simple tasks in a small workspace. The development of dedicated ultrafast vision sensors and associated closed-loop control schemes will allow us to track microobjects with robustness in a large workspace above 1 kHz sampling and will lead to more pertinent and complex applications in this field of research.

Nowadays, fast measurements in microrobotics are commonly taken by a photodiode or quadrant. Their performances are often limited to a resolution of one or four pixels, which indicate reduced working distance and sensor alignment constraint. Multiobject tracking is only possible with video cameras. Although very high speed cameras exist (up to 30 kHz at full resolution), they remain an offline solution because large amounts of data are stored in a local memory and processed offline (Keen *et al.,* 2007). Recently, rapid CMOS cameras have been developed allowing a reduction of the region of interest. They can transmit the image in real time (Gibson *et al.,* 2008), but the entire frame online processing remains time consuming. To overcome these limitations, dedicated image processing hardware (e.g. FPGA) (Saunter *et al.,* 2005) or 'smart' CMOS cameras with on-chip processing (Constandinou & Toumazou, 2006; Fish *et al.,* 2007) are used, but these add extra expenses, development cycles and the requirement of specific hardware knowledge. Current real-time multiple-particle tracking algorithms are often limited to the centre of mass with limited performances if scenes are cluttered.

Since the pioneering work on the address-event representation (AER) vision system (Mahowald, 1992), the performance of the latest developed neuromorphic bioinspired retinas allows us to consider a new paradigm in visual computation sensors (Delbruck, 2008; Lichtsteiner *et al.,* 2008). The trigger for a pixel read-out, or send-out, can be chosen as a threshold on its activity changes. Unlike the work of Mallik (Mallik *et al.,* 2005), which also relies on recording temporal changes, the presenting paradigm insist on that

Correspondence to: Stéphane Régnier, Institut des Systèmes Intelligents et de Robotique, UPMC, CNRS UMR-7222, 4 place Jussieu, CC 173, 75252 Paris cedex 05, France. Tel: +33 (0) 1 44 27 28 79 33; fax: +33 (0)1 44 27 51 45; e-mail: regnier@isir.upmc.fr.

**Table 1.** Comparison of fast vision solutions in micromanipulation.

| Type | Price (k€) | Acquisition (kHz) | Processing (kHz) | Region of interest | Comment |
|---|---|---|---|---|---|
| Photodiode [1] | 0.2 | 10[a] | 10[a] | 2 × 2 | Only single sphere, difficult to align |
| Ultrafast cam [2] | 30 | 30+ | offline | Not detailed | Not for real time use |
| CMOS [3] | 1.5 | 1 | 0.5 | 40 × 40 | Image processing with a PC |
| CMOS + hardware [4] | 3–4 | 5 | 5 | 100 × 100 | Special hardware required |
| AER [5] | 2 | 1000[a] | 30[b] | 128 × 128 | High speed and low consumption |

[a] These frequencies are the information refreshing rate, at the contrary of classical frame-based cameras' rates.
[b] To be achieved in this paper.
[1][2] Keen *et al.,* 2007, [3] Gibson *et al.,* 2008, [4] Otto *et al.,* 2008, [5] Lichtsteiner *et al.,* 2008.

pixels collect and send their own data as local information independently of the others, thus freed from frames. The collected data include the spatial location of active pixels and an accurate time stamping at which a change occurs above a threshold. Additional information such as polarity of events (positive or negative change of light) can be added (Zaghloul *et al.,* 2003). Computationally, this representation differs from frames as it encodes the data in a compressed form of event streams, the events can then be processed locally while encoding the additional temporal dynamics of the scene.

These sensors have been recently used in vehicle detection (Litzenberger *et al.,* 2006a,b) and incidents' detections (Fu *et al.,* 2008). Perhaps, the most convincing real-time achievement can be found in the academic pencil balancing experiment which relies on lines' detection for tracking (Conradt *et al.,* 2009). Table 1 gives a summary of the above-described vision systems' prices and experimental performances; it also shows the clear advantage of the use of asynchronous AER.

This paper implements a real-time vision application using asynchronous event-based retinas applied for the first time to the microworld conditions. The carried-out work uses an asynchronous event-based Hough transform to detect circles. The adapted technique is able to detect a single microsphere's position at an equivalent frequency of 30 kHz or multiple microspheres at several kHz. Finally, a high speed real-time Brownian motion tracking is implemented with a subpixel precision. The presented experiments will show that it outperforms existing conventional microparticle tracking techniques.

## Asynchronous event-based vision

Biological retinas, unlike frame-based cameras, transmit less-redundant information about a visual scene in an asynchronous manner. The various functionalities of the retina have been incorporated into neuromorphic vision sensors since the late 1980s in the pioneering work of Mahowald (1992).

Since then, the most interesting achievements in neuromorphic retinas have been the development of activity-driven sensing. The event-based vision sensors output compressed digital data in the form of events, removing redundancy, reducing latency and increasing dynamic range compared with conventional imagers. A complete review of the history and existing sensors can be found in Delbruck *et al.* (2010). The dynamic vision sensor (DVS) used in this work is an AER silicon retina with 128 × 128 pixels (Lichtsteiner *et al.,* 2008). The DVS output consists of asynchronous address events that signal scene reflectance changes at the times they occur. Each pixel is independent and detects changes in log intensity larger than a threshold since the last event it emitted (typically 15% contrast). When the change in log intensity exceeds a set threshold, an ON or OFF event is generated by the pixel depending on whether the log intensity increased or decreased, see Figure 1. Since the DVS is not clocked like conventional cameras, the timing of events can be conveyed with an accurate temporal resolution of approximately 1 $\mu$s. Thus, the 'effective frame rate' is typically several kHz.

### *Notations and basic theories*

The DVS models the transient responses of the retina (Roska and Werblin, 2003). The stream of events from the retina can be defined mathematically as follows: let $Ev(x,y,t)$ be an event occurring at time $t$ at the spatial location $(x, y)^T$.

The values $Ev(x,y,t)$ are set to be $-1$ or $+1$ when a negative or a positive change of contrast is detected, respectively. We can then define $S_{t_k}$ as the set of points generating events at timestamp $t_k$:

$$S_{t_k} = \{(x, y) \mid \exists\, E\, v(x, y, t_k)\}. \quad (1)$$

The absence of events when no change of contrast is detected implies that redundant visual information usually recorded in frames is not carried in the stream of events.

### *Asynchronous hough circle transform*

The detection of microspheres is performed using the Hough transform (Hough, 1959). This technique is known to be robust even if observed scenes contain nonperfect circular objects. The method is considered to be computationally

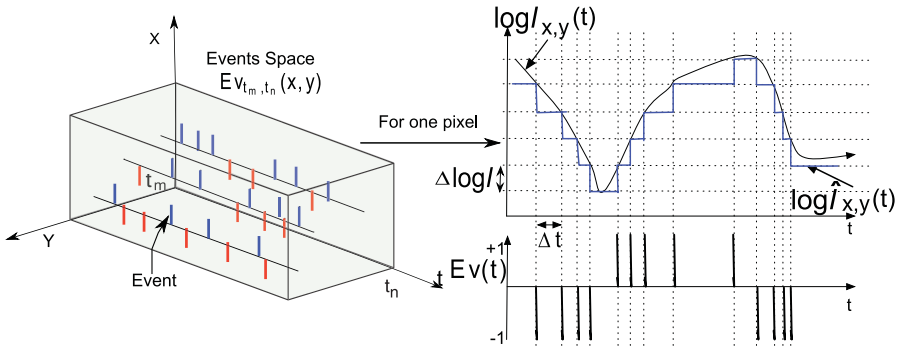


**Fig. 1.** Illustration of event space and quantification of pixels' grey-level variations into temporal contrast events. $\log \hat{I}_{x,y}$ is the step constant function which approximates $\log I_{x,y}$.

expensive; however, the sparse data produced by frame-free event-based cameras and their temporal asynchrony allow us to run it in real time.

Micromanipulation is generally performed in almost predetermined environments. Microspheres of the same size are used and their radius is known to users. If the radius $R$ is known, only their centre coordinates $(x_c, y_c)^T$ must be determined; in this case we are then dealing with a 2D Hough space. If the radiuses are different or unknown to users, the event-based Hough should be logically performed in a 3D space $(x_c, y_c, R)$. The event-based Hough transform using asynchronous events can then be defined:

$$H : S_{t_k} \mapsto A_k = H(S_{t_k}), \tag{2}$$

where $A_k$ is in case of two parameters search an integer matrix satisfying

$$A_k(i, j) \begin{cases} = 1 & \text{if } (x-i)^2 + (y-j)^2 = R^2 \\ = 0 & \text{otherwise} \end{cases}, \quad \text{for } \forall i, j \in [1,128], (x, y) \in S_{t_k}. \tag{3}$$

A first-in first-out (FIFO) data structure of size $l$ is set. The Hough space voted by all the incoming events in the FIFO can be expressed as $H(S_{t_{n-l+1}t_{n+1}})$, $t_{n+1}$is the current time. The general algorithm is given using the following recursive formula, called Continuous Hough hereafter:

$$H(S_{t_{n-l+1}t_{n+1}}) = H(S_{t_{n-l}t_n}) + H(S_{t_{n+1}}) - H(S_{t_{n-l}}), \tag{4}$$

with the convention $H(S_{t_{n-l}t_n}) = \sum_{t_{n-l}}^{t_n} H(S_{t_k})$. Afterwards, the circle centre $(x_c, y_c)^T$ can be detected simply by selecting the local maximum in Hough space. In applications where the object movement is subtle, like the Brownian motion detection, the resolution is generally too coarse for a precise analysis. In order to achieve subpixel resolution, a centre-of-mass algorithm (referred to as Centroid) within the neighborhood of the peak in Hough space can be calculated instead of choosing only the local maximum.

In real applications, more practical issues should be considered. A region of interest (ROI) should be set for each particle. Moreover, to dynamically track all the moving particles in the scene, their appearance or disappearance should also be detected in real time by setting corresponding thresholds and ensuring a boundary checking during each iteration. For illustration, the event-based Hough circle algorithm with Centroid is summarized in Algorithm 1.

**Algorithm 1** Event-based Hough circle tracking with fixed radius.

**Require:** $Ev(x, y, t_i), \forall i > 0$ **Ensure:** The position of circle centre $x_c, y_c$

1: Initialize the parameters
2: **while** an incoming new event $Ev(x, y, t_{n+1})$ **do**
3: Apply Equation (4)
4: **if** $(x, y) \in$ one of the ROIs **then**
5: Update the centre of the particle by applying centroid.
6: **else if** $(x, y) \notin$ ROIs **then**
7: Detect a new local maxima close to$(x, y)$, then using centroid to calculate a possibly new particle.
8: **end if**
9: Threshold and boundary checking.
10: **end while**

## Results

In this section, the experimental results will be presented in two stages. The first part uses a micromanipulation robot, where the equipped microstage moves several microspheres. In the second part, an experiment is shown to detect Brownian motions where the movements appear fast and small. This is an example of phenomena difficult to track in microworld.

### *Microsphere tracking*

In the first microrobotic experiments, thousands of microspheres with a constant diameter of 10 $\mu$m are tracked under $\times$ 20 magnification. The field of view contains a mean value of 50 microspheres moving simultaneously. The AER

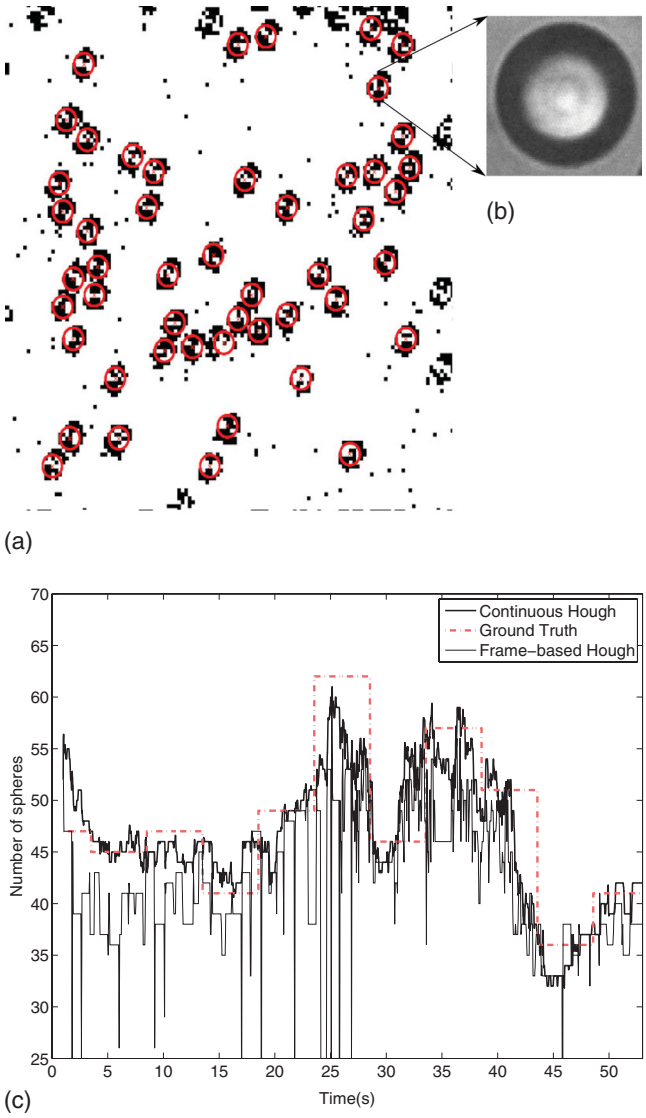


**Fig. 2.** (a) A multiple microspheres (10 $\mu$m) detection example. Black dots are the events in the FIFO. The red circles are the detected microspheres. (b) An image of one microsphere taken by the classical camera. (c) This figure compares the number of microspheres detected over time using the frame-based (green) and the event-based Hough (black) transform with an asynchronous AER retina. The microspheres are counted manually every 5 s (the red envelope).

retina threshold is adjusted manually to our experimental condition for a better detection.

In Figure 2(a), a screen view shows a frame obtained by summing events over a time window representing the activity of all pixels stored in the FIFO. The FIFO size is set to a maximal size of 2000 events. As shown in Figure 2(a), the algorithm is capable of detecting several dozens of moving microspheres simultaneously. It is important to point out that only the activities of pixels are taken into account; therefore, the polarity does not have an impact on the computational process of the application. The ground truth envelope corresponding to the number of microspheres manually counted every 5 s (Fig. 2(c)) shows that the method does not suffer any loss. A frame-based Hough using accumulation maps of events from the asynchronous AER retina has been implemented to provide comparison. The sudden drop in the circle number of the frame-based Hough is due to the discrete motions of the microspheres. When the microstage stops, it causes a sudden burst of noise that the frame-based Hough technique cannot handle without a robust tracking filter. The event-based Continuous Hough overcomes this problem due to its quick 'update from last position' mechanism, which acts intrinsically as a tracking filter (see Eq. (4)).

Further experiments are fulfilled for real-time microrobotic applications. The system setup is presented in the experimental section. The program implemented in C++ under Windows was running online. The microspheres used were of known radius of 6 $\mu$m while the magnification was set to $\times$100. The results of real-time experiments are shown in Figure 3(a) where three microspheres are moving in the water current. The update rate is shown in Figure 3(b). From this figure, the mean time for processing an event is about 32.5 $\mu$s, namely 30 kHz frequency in C++. If the events are distributed over three circle edges, the detection of each microsphere's position can then be computed at a mean frequency close to 10 kHz.

It is important to emphasize that no specific hardware was used except for the AER retina. The experiment relied on an off-the-shelf 2.9 GHz Dual core desktop PC for the whole system running four threads, including the microstage control, with a total CPU load little more than 50% of its power and a memory consumption of about 4 MB. If compared to frame-based techniques, in terms of rapidity, memory consumption and hardware price, event-based vision outperforms frame-based vision by far. It is also important to point out that the used event-based method is a much more complex algorithm than the classical centre-of-mass method.

Compared to pure tracking of events that have been reported in Delbruck & Lichtsteiner (2007), the computational load of the Hough method is higher (five times) as it is aimed to detect specific shapes while in Delbruck & Lichsteiner (2007), the algorithm is tracking blobs of events regardless to shapes. Introducing a constraint on the tracked shapes ensures that in case of several moving objects, only spheres will be detected. This introduces stability in the measurements as usually needed in micromanipulation.

### *Brownian motion detection*

Brownian motion corresponds to the thermal agitation of micro/nanosized particles in the fluid. The theoretical displacement of the particle satisfies a centred normal distribution. The standard deviation depends on the temperature, viscosity parameter and the sampling frequency in a synchronous sampling mode (Crocker & Grier, 1996); in our condition, 70% of the measurements are smaller than

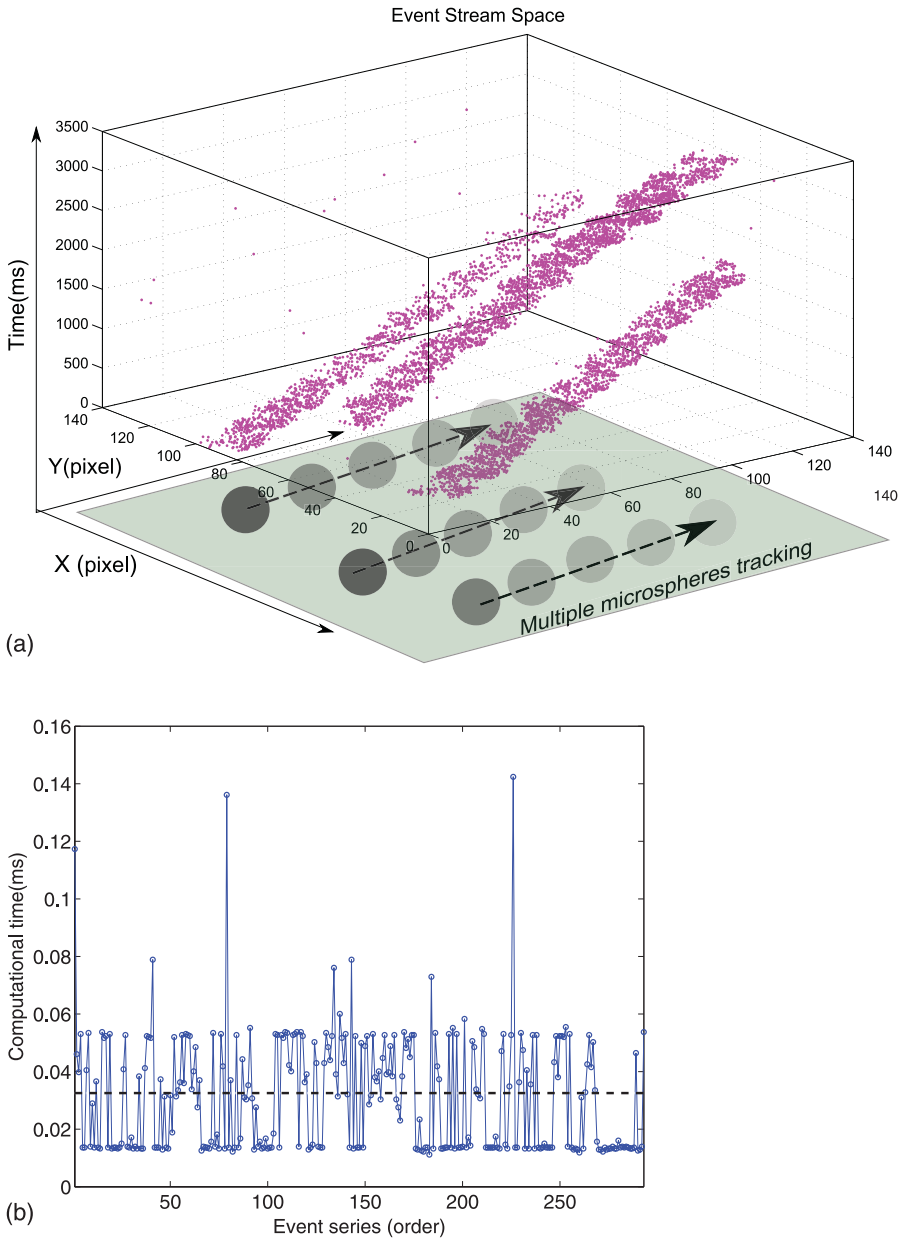


**Fig. 3.** (a) Event space of fast moving circles influenced by water current, whose positions are detected in real time. The vertical axis is the time; the other two are the $xy$ plane. Noise can be observed; however, our algorithm is very robust to overcome temporally unrelated noise. (b) Time consumption in a real-time test. The mean time for processing an event is at about 32.5 $\mu$s (dot line), namely 30 kHz frequency. The peaks are caused by the OS interruptions.

2 nm. The position signal behaves like a white Gaussian noise and has a large frequency spectrum. This phenomenon is ideal to test the sensitivity and dynamics of the presented system.

A 2.7-$\mu$m microsphere's trajectory is plotted in Figure 4 with and without the Centroid algorithm applied. The precision is improved by the use of the Centroid algorithm; it allows a subpixel accuracy (1 pixel = 0.19 $\mu$m, for the $\times$100 objective). Figure 5 shows the spatial distribution of the microsphere's positions detected by the Continuous Hough. The pattern results from an angular sampling step of 5° used for the Hough accumulator. The chosen sampling value is the best experimental compromise for rapidity and precision. Figure 6(a) shows the amplitude $\Delta r = (\Delta x^2 + \Delta y^2)^{1/2}$ of the Brownian motion measurements compared to the theoretical distribution. The standard deviation of our measurement along the $x$, $y$ axes is $\sigma_x = 1.53$ nm, $\sigma_y = 1.59$ nm, respectively. An incomplete Gaussian is obtained

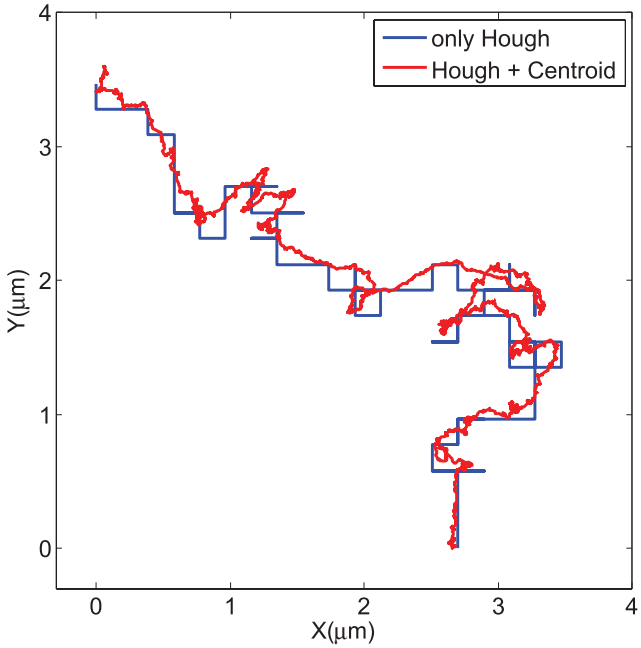


**Fig. 4.** Comparison of the detection results (Cartesian coordinates) by using only Continuous Hough and by combination of Hough and Centroid. With only Hough, the result has pixel accuracy, whereas with the latter method, a subpixel resolution can be achieved.

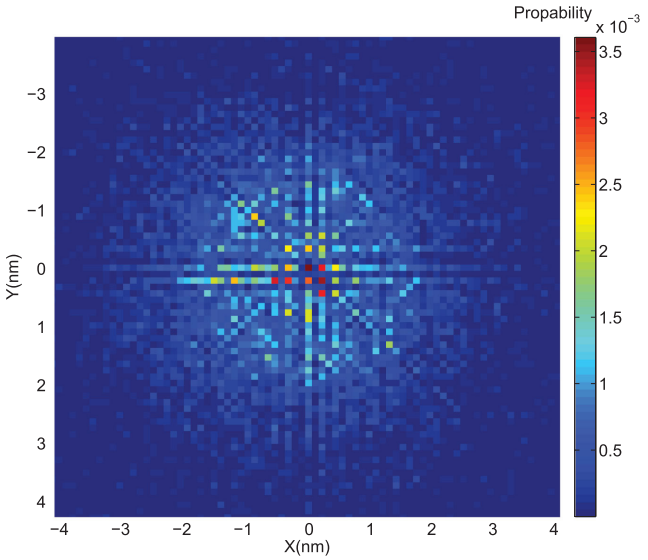


**Fig. 5.** The displacement $(\Delta x,\ \Delta y)^{\mathrm{T}}$ distribution of a microsphere's Brownian motion. This is a top view of the Gaussian distribution with a standard deviation of $\sigma_x = 1.53$ nm, $\sigma_y = 1.59$ nm. The colour axis represents the probability counts in each location. Note that the result is more sensible around the voting angle in Continuous Hough transform.

since too small displacements cannot be optically measured. The lower boundary to consider the measurements as being accurate is equal to the maximum of the distribution shown in Figure 6(a) (which is experimentally measured to 1.9 nm). Figure 6(b) shows the distribution calculated by the frame-based Hough for comparison. Frames are obtained by accumulating events to simulate a high speed CMOS camera of frame frequency 1 kHz. By also applying a Centroid after the Hough, the method is able to track a single microsphere with subpixel resolution offline. The measured standard deviation of the frame-based Hough in Figure 6(b) is 35 nm. Compared to Figure 6(a), this deviation is significantly larger due to the lower sampling frequency. The distribution is also coarser since less temporal correlation information is used by the frame-based Hough.

The bandwidth of AER retinas is not limited by any frame rate constraints due to its asynchronous principle. As shown in the work of Lichtsteiner *et al.* (2008), the temporal resolution limit is set by the minimum timestamp which is 1 $\mu$s and the pixel bandwidth which is up to 3 kHz. The AER Brownian motions' measurements have a mean temporal resolution of 2.15 $\mu$s.

### *Further considerations and optimization*

The selection of events only in the circle's ROI allows eliminating the influence of the fixed-pattern noise. The Hough algorithm itself is also very robust to noise, because only the dominating value in the Hough space will be taken into account for the final decision of the sphere centre.

Concerning the system latency, AER events are sent in the form of packet through the USB interface. By choosing an optimal device interrupt polling interval, the latency of the system can be achieved at the level of $2.8 \pm 0.5$ ms (Delbruck & Lichsteiner, 2007). This is fast enough for the control of microsystems in closed loop (Ivan *et al.*, 2011).

Moreover, the FIFO size is an important parameter that must be tuned accurately. If the FIFO size is too small, the peaks values are not highlighted in the Hough space leading to false alarms. On the contrary, the accumulated values around the particle centre are too important; a large inertia is then introduced and causes an apparent detection's delay. In our experiment of multiple particles' tracking, the size has been experimentally set to 2000 events. For Brownian motion detection where events' generation rates are much lower, the size around 700 is optimal considering the general performance. This value is largely dependent on the complexity of the scene, like the number of microspheres. More complex dynamic management of FIFO can also be used.

## Discussion

Due to the high dynamics at the microscopic scale, fast position detection and tracking is a key problem for many applications like micromanipulation, *in situ* force sensing and mechanical biological characterization. High bandwidth and sensitivity sensors help to stabilize automated systems and subsequently

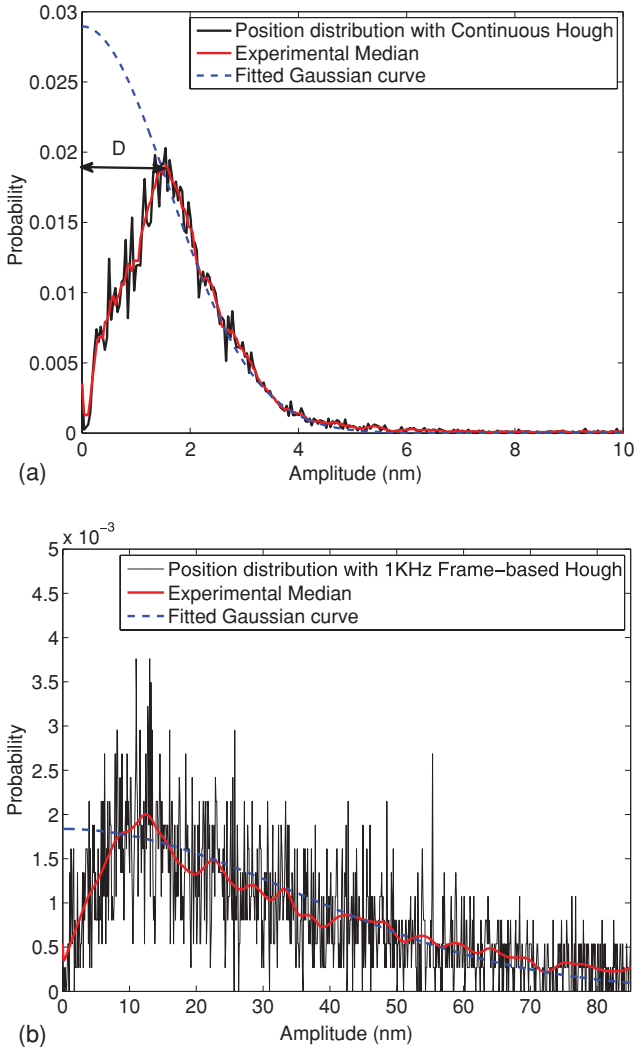


**Fig. 6.** (a) The particle relative displacement distribution $(\Delta x^2 + \Delta y^2)^{1/2}$ (in black) and the fitted Gaussian envelope (in blue). The red curve is the experimental median. The camera does not reliably detect low displacements below 0.01 pixel (D). The standard deviation of the fitted Gaussian curve is 1.6 nm. (b) The same displacement distribution obtained from Frame-based Hough. Frames are obtained by accumulating events to simulate a high speed CMOS camera of frequency 1 kHz. The centroid algorithm is applied after the Hough. The standard deviation of the fitted Gaussian curve (blue) is 35 nm.

to handle fragile microobjects. This is well suited for lab-on-a-chip issues. The development presented in this paper demonstrates a real-time multi-micro-objects detection with a frequency of up to 30 kHz and its application to the detection of Brownian motion. The asynchronous event-based acquisition and derived methods outclass existing micromanipulation methods relying on CMOS or ultrafast cameras.

Asynchronous event-based representation is a new optimal solution for ultrafast sensing. At the contrary of conventional image processing methods, it does not operate on the entire frame, dealing with each pixel many times and leading to a high cost of computation and memory communication bandwidth, especially for high frame rate applications. This work shows that asynchronous event-based retinas have an unprecedented raw performance potential, characteristics and usability. Although the presented method has been developed as a software algorithms running on a standard PC platform, it seems obvious that its implementation in embedded hardware will reach even much higher performances. These sensors are very recent; they have substantial space for innovation and the potential of realization of small, fast, low power embedded sensory-motor processing systems that are beyond the reach of current frame-based techniques.

Recent developments in the field of neuromorphic sensing show that an evolution of the chip already exists and is able to record the true luminance information (Posch *et al.*, 2010). However, the most important hindrance for the use of this camera lies in the fact that it is very original and not still fully understood. The developed off-the-shelf image and vision algorithms are not directly applicable but seem to be easily adaptable. It is therefore expected that these sensors should in the very near future have a strong impact on the domain of micro/nanorobotics and physics.

## Conclusions

In this paper, an event-based Hough circle transform has been developed. It overcomes problems often met in classical frame-based processing where redundant information leads to low speed processing. The use of asynchronous acquisition of the local luminance changes in the form of address events streams is still in early stage. It allows us to consider new perspectives to fast computation in microrobotics. In the future, it is expected that more complex event-based algorithms can be developed. Existing techniques can easily be adapted to different micromanipulation tools, such as optical or magnetic tweezers, different tasks like nanotubes, biological cells, DNA handling, etc.

## Experimental details

Our experimental system is plotted in Figure 7. The light beam is projected from above and the microscope objective (×20/NA.0.25 or ×100/NA.0.8, Olympus, Japan) is placed upside down to observe samples in the Petri dish. The Petri dish is placed inside a chamber equipped with a thermal-coupled temperature controller. The platform is a controllable microstage driven by a DC-Servo Motor Controller (C-843, Physics Instrument, Germany). The light beam is split into two parts and redirected separately to the AER retina (DVS, ETH, Switzerland) and to a classic CMOS camera (Basler, Germany). The two cameras are aligned to produce the same view of the microscope. The CMOS camera is used to provide a visual

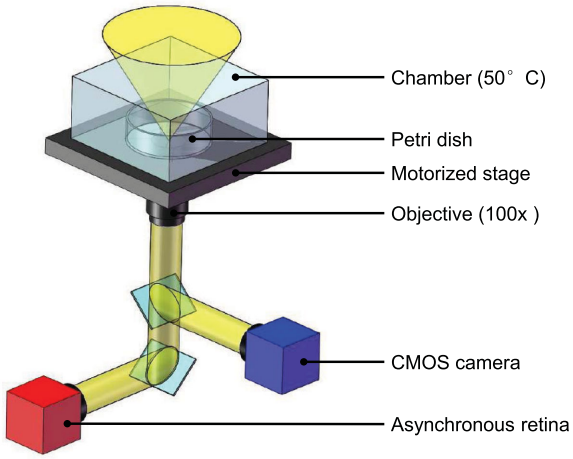


**Fig. 7.** A brief illustration of our experimental setup.

feedback for the system's control and direct monitoring of the AER retina.

Polystyrene microspheres (Polysciences, Warrington, PA, U.S.A.) of sizes 6, 10 and 20 $\mu$m are used for microrobotics applications and a size of 2.7 $\mu$m for the Brownian motions' detection. They are placed in pure water. In the Brownian motions' detection experiment, the chamber temperature is controlled at around 50 °C.

## References


Bolopion, A., Xie, H., Haliyo, S. & Régnier, S. (2010) Haptic teleoperation for 3D microassembly of spherical objects. *IEEE/ASME Trans. Mechatron.* **99,** 1–12.

Conradt, J., Berner, R., Cook, M. & Delbruck, T. (2009) An embedded AER dynamic vision sensor for low-latency pole balancing. *Fifth IEEE Workshop on Embedded Computer Vision*, Kyoto, Japan.

Constandinou, T.G. & Toumazou, C. (2006) A micropower centroiding vision processor. *IEEE J. Solid-State Circuits.* **41,** 1430–1443.

Crocker, J.C. & Grier, D.G. (1996) Methods of digital video microscopy for colloidal studies. *J. Colloid Interface Sci.* **179,** 298–310.

Delbruck, T. & Lichtsteiner, P. (2007) Fast sensory motor control based on event-based hybrid neuromorphic-procedural system. *IEEE International Symposium on Circuits and Systems*, pp. 845–848.

Delbruck, T. (2008) Frame-free dynamic digital vision. *International. Symposium on Secure-Life Electronics*, Tokyo, Japan, pp. 21–26.

Delbruck, T., Linares-Barranco, B., Culurciello, E. & Posch, C. (2010) Activity-driven, event-based vision sensors. *IEEE International. Symposium on Circuits and Systems*, pp. 2426–2429.

Fish, A., Sudakov-Boreysha, L. & Yadid-Pecht, O. (2007) Low-power tracking image sensor based on biological models of attention. *Int. J. Information Theories and Applications.***14,** 103–114.

Fu, Z., Delbruck, T., Lichtsteiner, P. & Culurciello, E. (2008) An address-event fall detector for assisted living applications. *IEEE Trans. Biomed. Circuits Syst.* **2,** 88–96.

Gibson, G., Leach, J., Keen, S., Wright, A.J. & Padgett, M. J. (2008) Measuring the accuracy of particle position and force in optical tweezers using high-speed video microscopy. *Opt. Express.* **16,** 14561–14570.

Hough, P.V.C. (1959) Machine analysis of bubble chamber pictures. *Proceedings International Conference On High Energy Accelerators and Instrumentation*, pp. 554–556.

Ivan, I., Hwang, G., Agnus, J., Rakotondrabe, M., Chaillet, N. & Régnier, S. (2011) First experiment on MagPieR: a planar wireless magnetic and piezoelectric microrobot. *IEEE International Conference on Robotics and Automation*, pp. 102–108.

Keen, S., Leach, J., Gibson, G., & Padgett, M.J. (2007) Comparison of a high-speed camera and a quadrant detector for measuring displacements in optical tweezers. *J. Opt. A: Pure Appl. Opt.* **9,** S264–S266.

Lichtsteiner, P., Posch, C. & Delbruck, T. (2008) A 128*128 120 db 15 us latency asynchronous temporal contrast vision sensor. *IEEE J. Solid-State Circuits.* **43,** 566–576.

Litzenberger, M., *et al.* (2006a) Estimation of vehicle speed based on asynchronous data from a silicon retina optical sensor. *IEEE Intel. Transport. Systems Conference*, pp. 653–658.

Litzenberger, M., Posch, C., Bauer, D., Belbachir, A., Schon, P., Kohn, B. & Garn, H. (2006b) Embedded vision system for real-time object tracking using an asynchronous transient vision sensor. *Twelfth Digital Signal Processing Workshop—Fourth Signal Processing Education Workshop*, pp. 173–178.

Mahowald, M. (1992) *VLSI analogs of neuronal visual processing: A synthesis of form and function.* PhD thesis, California Institute of Technology, Pasadena, CA.

Mallik, U., Clapp, M., Choi, E., Cauwenberghs, G. & Etienne-Cummings, R. (2005) Temporal change threshold detection imager. *Solid-State Circuits Conf*, pp. 362–363.

Otto, O., Gutsche, C., Kremer, F. & Keyser U. F. (2008) Optical tweezers with 2.5 kHz bandwidth video detection for single-colloid electrophoresis. *Rev. Sci. Instrum.* **79,** 023710.

Pacoret, C., Bergander, A. & Régnier, S. (2010). Haptic feedback of piconewton interactions with optical tweezers. *Eurohaptics*, pp. 333–338.

Pacoret, C., *et al.* (2009) Touching the microworld with force-feedback optical tweezers. *Opt. Express* **12,** 10260.

Posch, C., *et al.* (2010) Asynchronous time-based image sensor (ATIS) camera with full-custom AE processor. *IEEE International Symposium on Circuits and Systems*, pp. 1392–1392.

Roska, B. & Werblin, F. (2003) Rapid global shifts in natural scenes block spiking in specific ganglion cell types. *Nature Neurosci.* **6,** 600–608.

Saunter, C.D., Love, G.D., Johns, M. & Holmes, J. (2005) FPGA technology for high speed, low cost adaptive optics. *International Workshop on Adaptative Optics for Industry and Medicine*. pp. 60181G.1–60181G.7.

Zaghloul, K.A., Boahen, K. & Demb, J.B. (2003) Different circuits for ON and OFF retinal ganglion cells cause different contrast sensitivities. *J. Neurosci.* **23,** 2645–2654.


## Supporting information

*Asynchronous event-based high speed vision for microparticle tracking*

Additional supporting information may be found in the online version of this paper:

**Video S1**: BrownianMotion.wmv—Brownian motion detection of a microsphere of size 2.7 $\mu$m in pure water. The timestamp in the up-left corner is in microsecond. The blue dots are event activities and the black circle is the detected microsphere.

Please note: Wiley-Blackwell are not responsible for the content or functionality of any supporting materials supplied by the authors. Any queries (other than missing material) should be directed to the corresponding author for the paper.